sustainability

MDPI

Article

Sustainable Energy Management and Control for Variable Load Conditions Using Improved Mayfly Optimization

Prabu Subramani [1], Sugadev Mani [2], Wen-Cheng Lai [3,4,*] and Dineshkumar Ramamurthy [5]

[1] Department of ECE, Mahendra Institute of Technology, Namakkal 637503, India; drsprabu@ieee.org
[2] Department of ECE, Sathyabama Institute of Science and Technology, Chennai 600119, India; sugadev.ece@sathyabama.ac.in
[3] Bachelor Program in Industrial Projects, National Yunlin University of Science and Technology, Douliu 640301, Taiwan
[4] Department of Electronic Engineering, National Yunlin University of Science and Technology, Douliu 640301, Taiwan
[5] Department of ECE, Kings Engineering College, Irungattukottai, Sriperumbudur 602117, India; dineshkumar@kingsedu.ac.in
* Correspondence: wenlai@yuntech.edu.tw or wenlai@mail.ntust.edu.tw

Abstract: In recent trends, renewable energies are infinite, safe, and are becoming a reliable source for electricity requirements. However, they have certain variations in their results because of climate change, which is its major issue. To solve this challenge, a hybrid renewable energy system was created by combining various energy sources. Energy management strategies must be employed to determine the best possible performance of renewable energy-based hybrid systems, as well as to fulfil demand and improve system efficiency. This work describes an Energy Management System (EMS) for a Hybrid Renewable Energy System (HRES) called Improved Mayfly Optimization-based Modified Perturb and Observe (IMO-MP&O). The developed EMS is based on basic conceptual constraints and has the goal of meeting the energy demand of connected load, ensuring energy flow stabilization, and optimizing battery utilization. In addition, the suggested IMO-MP&O can identify the condition and operating state of every HRES sub-system and assure the network stability of frequency and voltage changes. Numerical simulations in the MATLAB/Simulink environment were used to evaluate the proposed EMS. The simulated results show that the proposed IMO-MP&O achieves the harmonic error of 0.77%, which is less than the existing Maximum Power Point Tracking (MPPT) control and Artificial Neural Network (ANN)-based Z-Source Converter methods.

Keywords: battery; energy management system; improved mayfly optimization; modified perturb and observe; photo-voltaic and wind turbine

Citation: Subramani, P.; Mani, S.; Lai, W.-C.; Ramamurthy, D. Sustainable Energy Management and Control for Variable Load Conditions Using Improved Mayfly Optimization. *Sustainability* **2022**, *14*, 6478. https://doi.org/10.3390/su14116478

Academic Editor: Grigorios L. Kyriakopoulos

Received: 11 May 2022
Accepted: 23 May 2022
Published: 25 May 2022

1. Introduction

Generally, solar, wind, geothermal power, and tidal energy are examples of renewable energy sources. These are regarded as infinite because they occur constantly and continually renew themselves [1,2]. Wind and solar power hold a special place among such energy sources. These resources are being studied more closely than other renewable sources [3] due to the presence of wind and sun all over the earth. The goal is not only to gather power but also to convert it to appropriate values, control the power that already exists, and eliminate the oscillations [4]. It is important to reduce the system's expenditure while controlling each of these resources [5]. The management of these components as a whole is significantly more difficult than controlling them independently. All distributed sources are managed separately and concurrently in a distributed mode because it completely depends on the operational circumstances and energy requirements [6]. PV systems can't provide constant power when the sun isn't shining [7]. Conversely, a wind farm will not function in the absence of wind [8]. In this scenario, the necessary energy should have the framework

to compensate for the absence of energy if the network does not function consistently or the combination generates less power than is needed [9]. Energy management ensures that the system runs smoothly and does not run out of energy in all the conditions [10]. The major goal is to acquire clean, long-lasting energy with a predictable frequency and voltage. Harmonic distortion should be strictly managed while or after the energy is obtained [11]. Renewable energy has been the sole source of contribution to global power generation capacity in recent years. HRES battery systems were created to improve system productivity and effectiveness by merging various voltage sources [12].

Renewable energy technology developments have increased efficiency while lowering costs [13]. Multiple studies on the best sizing of a PV/wind hybrid energy storage system have been conducted by altering the PV gradient and hub height to analyze the environmental practices of substitute arrangements [14]. If there is no sunlight or cold air, it is critical to keep the rechargeable battery packs charged. There will be no energy in the device without battery backup. As mentioned earlier, integrating wind and solar renewable resources will increase total energy generation [15]. Furthermore, to provide a steady electricity supply, and also to substitute for every deficit in renewable power, a battery storage framework was designed. In contemporary research, battery management devices are primarily utilized [16]. The majority of hybrid systems have unique designs; however, a complete examination of hybrid systems takes a long time and is expensive. The required time & expense for the simulation process were also provided [17], even though it is difficult to research all the solutions. Customers will be confused if a given process does not match the predicted computational results [18,19]. The improved mayfly optimization technique is established here by including a weighting factor to control the process, which results in the best possible outcome. Modified Perturb and Observe is utilized to alleviate the drift issue that causes the extracted power to oscillate. The presented IMO-MP&O control takes into account load side instability, non-linear design and controlling functions on load generator sides. The study contributions are as follows:

- Usage of RES in conjunction with a battery reduces operating costs since batteries are inexpensive, enhancing their adaptability. As a result, by inserting the batteries into the system, a higher energy density is produced.
- The improved mayfly optimization-based MP&O optimized the step size and produced the required duty cycle ratios due to the overall decrease in step size in the exploitation stage. The corrected duty cycle ratio provides a greater voltage to alleviate the overvoltage problems in the grid.
- The IMO and MP&O methods are intended to create an efficient EMS that can meet the ever-increasing load needs. By activating the converter switching, IMO is utilized to manage the wind/battery and generate steady energy.
- The expense of an IMO-MP&O method with grid-connected RES is calculated using different temperature and illumination levels.

The following is the organization of this research paper: Section 2 describes a literature review of the current studies on the PV/wind/battery system. Section 3 discusses the challenges with the PV/wind/battery system. Section 4 discussed the objectives of this research. The modelling of the PV system, wind farm and the battery is presented in Section 5. In Section 6 the projected EMS method using IMO and MP&O is described. In Section 7, the simulation and analytical findings of IMO-MP&O are provided. The conclusion of this study is given in Section 8.

2. Literature Review

Azaroual, M. Ouassaid, and M. Maaroufi [20] used a Time of Use (ToU) tariff and step rate to demonstrate appropriate EMS among PV, Wind, and Battery. ToU tariffs are considered in the analysis to manage utility grid performance and to account for power price fluctuations. As a result, two energy management approaches have been created in order to alter tariffs for maximum benefit. Different home Feed-in Tariffs (FIT) are being installed in order to maximize cost-saving and profit potential. For research verification, a standard

Moroccan house with a grid integrated PV-WT-Battery was employed. Despite the fact that it was an imbalance in minimizing the overall price and integrating power production.

Alaaeldin M. Abdelshafy et al. [21] demonstrated an improved EMS for a grid-connected Double Storage System (DSS) using PV, Wind, and Battery. A unique energy management method for the DSS is offered to increase system efficiency. The technique is based on a factor that is tuned for the DSS charging period. A Non-dominated Sorting Genetic Algorithm is used to find the challenge of optimal system design (NSGA-II). The multi-objective formula takes into account both the lowest capital costs and the lowest emissions. The recommended strategy's success was evaluated in terms of system financial and economic activities. They could not operate under light loads due to the pump and turbine working range.

The ideal architecture among hybrid PV, Wind, and Battery in distant places has been proposed by Hemeida, A.M et al. [22]. The suggested HRES has been optimized using the linear TORSCHE optimization method. Specific PV and wind configurations with battery have been assessed and compared to hybrid sources. Linear TORSCHE assists in determining the optimal size for all components in the hybrid system, providing adequate energy to be generated for off-grid loads. The effectiveness and dependability of such a system have been proven through cost efficiency assessment. However, for maintenance and operation, wind energy requires competent standards.

Elkazaz et al. [23] introduced the EMS as a means of decreasing the microgrid's actual running costs while increasing RES self-dissipation. This self-dissipation was calculated by determining the best site for a battery based on price factors. The designed EMS features 2 levels: an upper control level and a bottom control layer. The higher layer employs the Convex Optimization Method, which resolves the planning issue and determines the objective criteria in a very short period. The derived samples were passed to the bottom control plane, which employs a regulator to locate the BESS in the best possible place. This paper makes no mention of frequency deviation that occurs throughout power transfer.

Jha and Kumar [24] developed a compensator for energy storage systems to help grid networks cope with rapid load changes. The battery's power supply was developed by developing an approach that also took into account the battery's level of charge (SOC). The battery's electricity was primarily determined by two factors: wind energy intensity and battery state of charge. The electricity was conserved by adding a voltage-dropping method into a DC-AC microgrid control mechanism. In addition, wind power was extracted using a generator that was regulated using the MPPT approach. This modulation technique only analyses the minimization of voltage plummeting when RES and storage technologies are used, and it ignores the EMS in the hybrid sources.

The integrated RES-dependent microgrid includes an appropriate regulator that was created by Padhmanabhaiyappan et al. [25]. The DC-DC converter was designed through an MPPT and also was deemed an advanced converter with a translation proportion. The Adaptive Whale Optimization Algorithm (AWOA) and Adaptive Neuro-Fuzzy Interference System (ANFIS) Scheme were used to manage the real and reactive power from the HCRDC-DC converter. AWOA was used to determine the proper modulation schemes for the power imbalance in both the demand and the generator. Furthermore, the AWOA data has been used to minimize the variance utilizing the ANFIS method. The converter employed in the microgrid requires one more additional capacitor to generate positive outcomes.

Satish Kumar et al. [26] presented an intelligent EMS for a modest combined wind-solar-battery-powered distribution network to evaluate the system state. For various operating situations, the basic objective is to provide continuous energy to the system. An EMS maintains the power imbalances for fluctuations in renewable power production as well as sudden load variances. However, the demand was maintained consistently to monitor the effectiveness of the renewable power conversion systems and the battery bank for fluctuations in the electricity produced by the RES; this would be harder to see if the demand was changing constantly.

For a smart DC-microgrid, Ahmad Aziz Al Alahmadi et al. [27] suggested a new resource management system based on fuzzy logic and fractional-order proportional-integral-derivative (FO-PID) regulator approaches. Battery, wind, and PV are among the hybrid forms of energy incorporated into a microgrid. The development of the intelligent FOPID method is designed to get the most power out of renewables while also improving the voltage stability delivered to the microgrid. The suggested controller guarantees that output power is steady and that operation was uninterrupted. On the other hand, the parameters vary constantly, which increases the computational cost.

Kavya Santhoshi et al. [28] showed ANN-based sustainable development of the power converter and battery in a grid-connected system fed through a switched Z source converter. Artificial Neural Network (ANN) was used to regulate battery energy to improve the battery's stability and longevity. Ultimately, the power at the common coupling node was supplied into an ANN-based space vector-modulated three-phase inverter, and the transformed AC power was fed into the grid. By evaluating the amount of synchronous control, the entire system performance can be determined. Variable input and load at the grid were used to verify that the suggested microgrid was reliable. However, the system has slow monitoring and service quality, as well as the inability to interact with a variety of situations.

Meenakshi De, G. Das, and K.K. Mandal [29] proposed an effective energy transfer control system for grid-connected PV system microgrids that included economic and operational planning. The Meta dynamic Flower Pollination Algorithm (MFPA) was provided in this paper for active voltage regulation in grid-connected systems incorporating cost-effective design. According to the findings, the expected FPA for grid production scheduling and energy control was extremely low. On the other hand, the results were produced with self-pollination activity, which was not optimum for intrinsic rearrangement.

3. Problem Formulation

To balance generated power among various sources for a grid integrated system, the following problem formulation is analyzed in this research. The multi-objective function is taken into account for the optimal sizing of generation, where usage and energy source facility are examined to optimize the total limitations. The following is an example of a problem formulation:

Load Generation Stability and Its Boundaries

The requirement for grid electricity is regulated by the electricity produced from diverse sources, according to Equation (1). The major constituent of current consumed by the load causes the power generating problem (grid). The output of PV & wind energy is unpredictable because of the unpredictable and discontinuous characteristics of solar and wind energy. As a result, the *SOC* (State of Charge) of the battery remains the major utility present in this article.

$$\sum_{k=1}^{N_k} P_{grid}(t) = \sum_{i=1}^{N_g} P_{Gi}(t) + \sum_{j=1}^{N_s} P_{Sj}(t) + P_{Ej}(t) \quad (1)$$

where the amounts of power switched by the grid at time t is designated as P_{grid}. The quantity of load level (grid) is characterized as k, g and s. The amount of load existent is stated as N_k. P_{Ej} signifies the battery storage power assigned for supply. P_{Gi} and P_{Sj} are quantities of output power from wind and solar.

Each factor comprising RES and battery backups contains lower and upper boundaries for their power generation, which are mentioned in Equation (2).

$$\begin{aligned} P_{Gi,min}(t) \leq\ & P_{Gi}(t) \leq P_{Gi,max}(t) \\ P_{Sj,min}(t) \leq\ & P_{Sj}(t) \leq P_{Sj,max}(t) \\ P_{Ej,min}(t) \leq\ & P_{Ej}(t) \leq P_{Ej,max}(t) \end{aligned} \quad (2)$$

Restrictions on charging and discharging proportions of battery are characterized as

$$SOC_{sj}(t) = SOC_{sj}(t-1) + P_{\frac{chg}{Dchg}}(t)$$
$$0 \leq \left| P_{\frac{chg}{Dchg}}(t) \right| \leq P_{CDsj,max} \quad (3)$$

where $SOC_{sj}(t)$ and $SOC_{sj}(t-1)$ are the charging amounts of a storage unit at the current and previous times, respectively. $P_{\frac{chg}{Dchg}}(t)$ is the charging (discharging) amount during the tth hour, and $P_{CDsj,max}$ signifies charging/discharging rate at maximum value. As a result, the hybrid energy system's output fluctuation is determined by placing a battery *SOC*. The balance between power requirements and surplus power is critical to power autonomy. A multi-source system is defined in this paper as a complicated system made up of various kinds of sources. The topic of finding the best energy distribution from various resources while also balancing load demand (grid) has been described as a multi-objective issue. To address multi-objective issues, a technique that depends on improved mayfly optimization-based MP&O is used to arrive at a general problem formulation.

4. Objectives

- A hybrid method name called improved mayfly optimization-based MP&O is applied to evaluate the EMS between renewable sources (solar and wind) and batteries at different load conditions;
- To assess the technical feasibility of a hybrid solar-wind power system to meet the load requirements;
- To evaluate a strategy for optimizing the size of the energy generation and storage (battery) subsystems;
- By extending the combination of the hybrid energy systems, to analyze the effect of load size or load variation.

5. Modelling of Energy Resources

5.1. Modelling of PV

The PV module is made up of open-circuit voltage, current, peak voltage and short-circuit current. The MPPT technology is utilized in the solar array to raise the Maximum Power Point [30]. Figure 1 shows the V-I characteristic of a PV cell [31]. From Figure 1, red color line denotes the power value at temperature 25 °C, where the blue color curve denotes the power value with respect to temperature 50 °C and 0 °C.

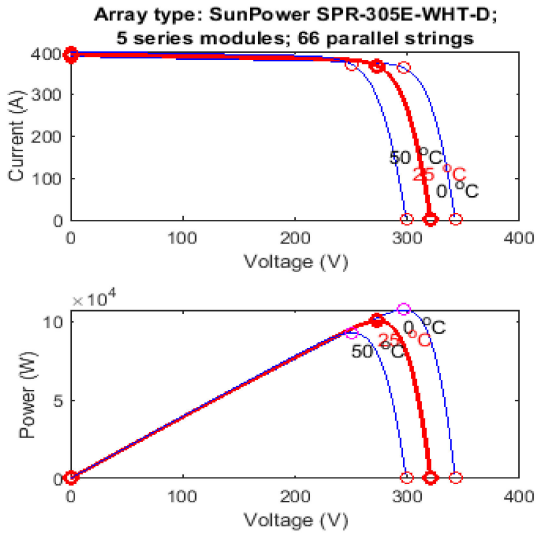

Figure 1. V-I characteristics of PV cell.

The following Equation (4) is used to identify the output power that depends on the I_M and V_M, which denote the maximum current and maximum voltage, respectively.

$$P_{MPPT}(t) = I_{MPPT}(t) \times V_{MPPT}(t) \tag{4}$$

The current and voltage of MPPT are given in Equations (5) and (6), respectively.

$$I_{MPPT}(t) = I_{SC}\left\{1 - C_1\left[exp\left(\frac{V_M}{C_2 \times V_{OC}}\right)\right]\right\} + \Delta I(t) \tag{5}$$

$$V_{MPPT}(t) = V_M + \mu V_{OC} \cdot \Delta T(t) \tag{6}$$

V_{OC} & I_{SC} is stated as open circuit voltage short circuit current; capacitances are represented as C_1 and C_2; the voltage at maximum level is designated as V_M; where C_1, C_2, $\Delta I(t)$ and $\Delta T(t)$ of (5) and (6) are stated in (7)–(10), respectively.

$$C_1 = \left(1 - \frac{I_M}{I_{SC}}\right) \times exp\left(-\frac{V_M}{C_2 \times V_{OC}}\right) \tag{7}$$

$$C_2 = \left(\frac{V_M}{V_{OC}} - 1\right) \times \left[\ln\left(1 - \frac{I_M}{I_{SC}}\right)\right]^{-1} \tag{8}$$

$$\Delta I(t) = I_{SC}\left(\frac{GT(t)}{G_{ref}} - 1\right) + \alpha_{1,sc} \times \Delta T(t) \tag{9}$$

$$\Delta T(t) = T_c(t) - T_{c,ref} \tag{10}$$

The current maximum value is designated as I_M; $T_{c,ref}$ states the cell temperature at a standard environment; the fixed standard of short circuit function is represented as $\alpha_{1,sc}$; T_c is characterized as cell temperature; $GT(t)$ represents the irradiation.

5.2. Wind Energy

The generation of wind is mostly caused by factors such as elevation, significant size, and speed [32]. Wind speed is measured by the voltage at the rated speed (V_{rs}), cut off voltage (V_{cf}), and cut in voltage (V_{ci}). Wind boundary conditions are primarily determined by speed and height. The wind direction, as per the wind shield, is not constant and changes with height. With an earth's atmosphere elevation of 1000 metres, a wind velocity of 14 metres per second is determined. In Equation (11), the wind output power is stated, including the boundary layer.

$$P_o = P_{rs}\left\{\begin{array}{cc} 0 & V < V_{ci} \\ a \times V^3 - b \times P_{rs}, & V_{ci} < V < V_{rs} \\ 1 & V_{rs} < V < V_{cf} \end{array}\right\} \tag{11}$$

P_o and P_{rs} signify output power and power at rated speed; where $a = P_{rs}/\left(V_{rs}^3 - V_{ci}^3\right)$ and $b = V_{ci}^3/\left(V_{rs}^3 - V_{ci}^3\right)$. The wind speed measurements are represented in Equation (12).

$$V_{hub} = V_0 \times \left(\frac{Z_{hub}}{Z_0}\right) \times \alpha \tag{12}$$

where V_{hub} states the height; V_0 signifies the reference speed; Z_{hub} represents the actual height; Z_0 states the speed limit and power is characterized as α.

5.3. Battery

Two semi-direct current and voltage estimation techniques are used to determine *SOC* that are simple and inexpensive to apply. As a result, one or both of them are frequently used in practical applications. Unfortunately, since none of these processes is accurate enough, other approaches must be utilized to enhance them. Because the battery *SOC* is

a critical quantity that indicates battery performance, accurate *SOC* estimation not only protects the battery and prevents overcharging or discharging but also extends its life. As a result, the ageing cycle procedure is used to examine *SOC* in terms of power value. The battery's charging and discharging conditions are represented in Equations (13) and (14). The battery is charged when the solar and wind exceeds the demand [33]. The process of discharge happens when the load exceeds the RES power levels.

$$SOC(t) = SOC(t-1) \times (1-\sigma) + [P_{RES}(t) - P_L(t)/\eta_{inv}] \times \eta_{ch} \quad (13)$$

$$SOC(t) = SOC(t-1) \times (1-\sigma) + [P_L(t)/\eta_{inv} - P_{RES}(t)] \times \eta_{disch} \quad (14)$$

$SOC(t)$ and $SOC(t-1)$ represent the charging and discharging conditions of the battery. The outflow rate is stated as σ. P_{RES} and P_L stand for power from RES and power from the load. η_{inv}, η_{ch} and η_{disch} are the efficiency symbols for the inverter, charging, and discharging states, respectively.

To determine an effective EMS, the technical performance of the battery must be assessed while considering forecasting errors caused by changes in the customer's load, intermittent renewable energy characteristics, and battery degradation. In this study, solar energy and weather factors are used to develop a mathematical model for PV arrays and wind models. Furthermore, battery degradation that occurs during charge and discharge cycles should be considered while evaluating the technical performance of the battery.

This research focuses upon battery degradation in self-consumption and searches for a connection to *SOC*. In this study, self-consumption is defined as charging the maximum PV generation and discharging the same amount of electricity to the load. Because the battery's *SOC* is strongly dependent on PV and load self-consumption, PV generation forecast is exploited to establish the battery's day-ahead schedule.

As a consequence, battery scheduling is implemented based on the superior forecasting model to charge the maximum amount of PV power and discharge for self-consumption of the consumer's load whenever PV generation stops. The cycle aging model estimates battery degradation after the charge and discharge cycles have been determined. Therefore, a control technique must be established to improve EMS and battery ageing without affecting the performance. In order to quantify the influence of battery degradation caused by PV charging, the cycle aging model is used in Equation (15), which is as follows,

$$Q_{cycle} = (\alpha SOC + \beta) \cdot \left(\frac{-E_a + \eta \cdot C_{rate}}{R_{gas} \cdot T_K} \right) Ah^2 \quad (15)$$

Fitting coefficients are declared as α and β; Compensation factor of C_{rate} is stated as η; Ambient Temperature is stated as T_K; Ah is declared as Ampere hour; Gas constant is represented as R_{gas}.

6. Proposed Method

This study develops many hybrid system strategies (solar energy, wind energy, and battery). It involves calculating load in various periods and seasons, gathering data on solar and wind speeds, constructing a hybrid renewable power system structure, and analyzing the parameter and pricing of system component elements. A composite renewable power generation network combines the generation and use of electrical power from many sources, as long as at least one of them is sustainable. To ensure energy security in the future, the country's energy resources must be diverse. To assure supply continuity, the energy mix must be rationalized, taking into account essential criteria such as economic cost, environmental impact, supply reliability, and consumer convenience.

The block diagram of the developed model is shown in Figure 2 [19]. While, the suggested controller receives power input from multiple HRES and loads. It provides the control factors with the necessary randomness while analyzing the input data, especially designed for investigating MPPT in a PV system with changing levels of illumination.

The suggested controller produces the necessary duty cycle after calculating those control factors that activate switches and restrict the peak energy drawn from the various resources. Grid voltage/frequency fluctuations are decreased when the control scheme is used. The proposed controller is used to manage the overall power and gives the decision to absorb or inject the reactive power to overcome the oscillation present in the system.

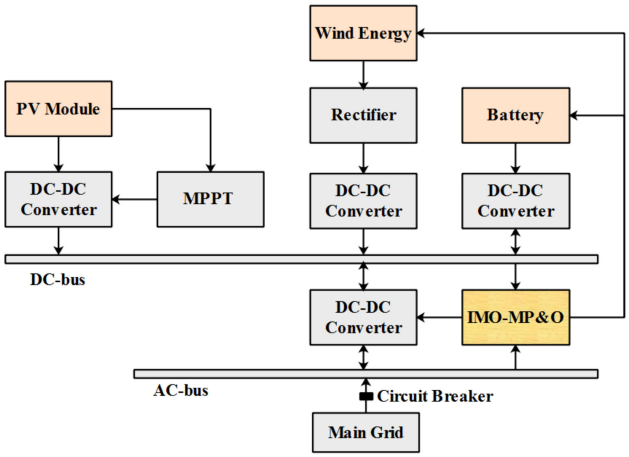

Figure 2. Block Diagram for the proposed method.

6.1. Mayfly Optimization Algorithm

The IMO is provided electricity to manage the ON/OFF condition of HRES. The duty cycle of IMO is used to specify the ON/OFF condition. Utilizing IMO in MPPT, the duty cycle is changed completely, unless there is a scheme to support MPP. The duty cycle used in the converter is specified by the inhabitants of IMO, and the result generated from IMO is the switching frequency that corresponds to fertility rate efficiency. The Mayfly algorithm is inspired by the natural activity of mayflies, particularly how they interact with one another. Mayflies are thought to be recognized individuals as quickly as they hatch from their eggs. Only the strongest mayflies typically live, regardless of their life span. Every mayfly has a ranking in the search space that correlates to a problem-solving method. In the traditional mayfly method, RAND function is used to generate novel parameters that contribute to local optimal results. Mayflies in swarms would be divided into male and female individuals for the MO method. Furthermore, because the male mayflies are constantly robust, they will be superior in enhancement. The parameters in the MO algorithm are the same as the PSO algorithm, as it adjusts their locations based on their existing positions $p_i(t)$ and velocity $v_i(t)$ at the present iteration count. All male and female mayflies would use Equation (16) to update their positions. Their velocity, on the other hand, would be updated in a variety of ways.

$$p_i(t+1) = p_i(t) + v_i(t+1) \tag{16}$$

6.1.1. Movements of Male Mayflies

Throughout cycles, male creatures in swarm intelligence could continue the exploring or subjugation process. The velocity would have been adjusted depending on the current fitness values $f(x_i)$ and the best fitness values in the past movements $f(x_{h_i})$.

If $f(x_i) > f(x_{h_i})$, the male mayflies' velocities would be updated based on their current velocities, the separation among them and the global optimal location, and the previous best movements are expressed in Equation (17):

$$v_i(t+1) = g \cdot v_i(t) + \alpha_1 e^{-\beta\gamma_p^2}\left[x_{h_i} - x_i(t)\right] + \alpha_2 e^{-\beta\gamma_g^2}\left[x_g - x_i(t)\right] \tag{17}$$

where g is stated as a variable that decreased exponentially from its peak to a reduced amount. The α_1, α_2 and β are used as constants to balance the values. The Cartesian

spacing among organisms and their previous best option, the global ideal position in swarm intelligence, is determined by the variables γ_p and γ_g. The distance array's next standard would have been the Cartesian distance, which is stated in Equation (18):

$$\|x_i - x_j\| = \sqrt{\sum_{k=1}^{n} \left(x_{ik} - x_{jk}\right)^2} \tag{18}$$

Alternatively, if $f(x_i) < f\left(x_{h_i}\right)$, the male mayflies could have been modernizing their rapidity from the present position through an unsystematic dance factor d, which is stated in Equation (19):

$$v_i(t+1) = g \cdot v_i(t) + d \cdot \gamma_1 \tag{19}$$

where the indiscriminate quantity in even dissemination and designation from the area $[-1, 1]$ are represented as γ_1.

6.1.2. Movements of Female Mayflies

Female mayflies should distinctively change their movements. Female mayflies have wings and have a short lifespan, ranging from 1 to 7 days; therefore, they would have been in a hurry to find male mayflies to engage with and procreate. As a result, they would change their velocities depending on which male mayflies they wanted to mate with.

The very first mate in the MO method should have been the finest female and male mayflies, and the second strongest female and male mayflies could have been the second mates, etc. As a result, in the ith female mayfly, $if\ f(y_i) < f(x_i)$, Equation (20) is stated as:

$$v_i(t+1) = g \cdot v_i(t) + \alpha_3 e^{-\beta \gamma_{mf}^2} [x_i(t) - y_i(t)] \tag{20}$$

where the alternative constant is stated as α_3, which is exploited to steady the quickness. The cartesian distance amongst them is signified as γ_m.

If $(y_i) < f(x_i)$, the female mayflies modify their velocities until the existing one runs through additional dance coefficients fl, which is expressed as (21)

$$v_i(t) = g \cdot v_i(t) + fl \cdot \gamma_2 \tag{21}$$

where the indiscriminate quantity in even dissemination and designated from the area $[-1, 1]$ is represented as γ_2.

6.1.3. Mating of Mayflies

Every one of the upper halves of female and male mayflies might be matched, and each of them can produce a couple of progeny. The crossover operator, as shown above, discusses the mating process between mayflies. Every parent is chosen from the male and female populations using the same estimation technique, namely the attractiveness of females to males. The parents might be chosen depending on their fitness functions or at random. The best female unites with the best male in terms of fitness, the second-best female with the second-best male, and so on. Their offspring might develop at a randomized rate from their mothers, which is expressed as (22) and (23),

$$offspring1 = L \times male + (1 - L) \times female \tag{22}$$

$$offspring2 = L \times female + (1 - L) \times male \tag{23}$$

An arbitrary statistic in Gauss distribution is stated as L; however, the mayfly optimization suffers from an initial tuning issue, so an additional weighted parameter is added to improve the efficiency. Therefore, improved mayfly optimization is proposed here to solve the multi-objective issues.

6.2. Improved MO Algorithm

Equations (19) and (21) indicate that employees in a swarm change their velocities at random in certain conditions. In the other cases, the velocities might be changed using efficient systems. Particular velocities were modified using Equations (17) and (20), which used weighted present velocities, including some additional weighted distance between them and previous best motions, the global best candidate, or their spouses. Equation (24) discovers whether halves of the balanced distance seem as follows:

$$v_p = \alpha_i e^{-\beta\gamma_j^2}\left(p_j - p_i\right) \tag{24}$$

If the distance among jth and ith individuals is extended, it appears that γ_j would be bigger. The weight might be reduced due to the slope of the negative upper bound. This implies that even if the distance between p_j and p_i is extended, the weights will drop, resulting in a reduction in the composited velocity v_p. Conversely, if the distance between p_j and p_i is reduced, the weights are enhanced accordingly. As a result, when p_j is far away from p_i, it updates its velocity with a smaller amplitude, whereas when p_j is close to p_i, it updates its velocity with a large magnitude. When people are far apart, they must increase their velocities with bigger levels, and while they are close together, they would maintain their velocities with reduced rates. As a result, Equation (24) must be improved to account for such a situation, as shown in the following Equation (25):

$$v_p = \alpha_i e^{-\frac{\beta}{\gamma_j}}\left(p_j - p_i\right) \tag{25}$$

The flowchart for the mayfly optimization algorithm is shown in Figure 3 [34].

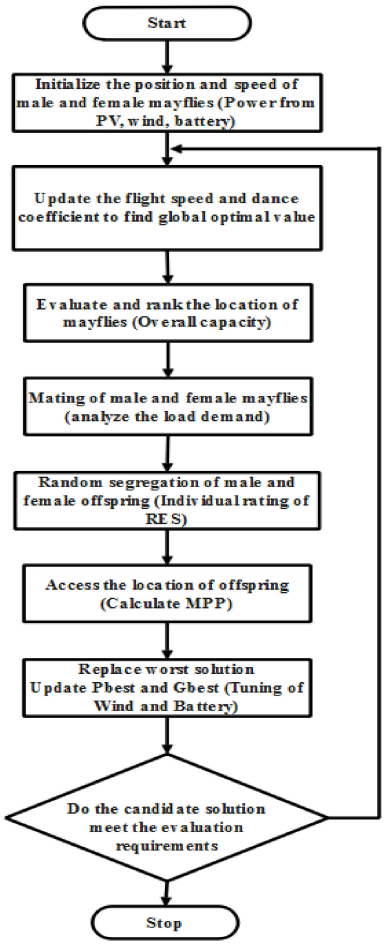

Figure 3. Flowchart for Mayfly Optimization.

6.3. Modified P&O Algorithm

In general, in the P&O algorithm, the results are affected by drift value. By including the information on a change in current & voltage (ΔI and ΔV), MP&O is projected to eliminate the drift issue. The drifting issue is fixed by including the ΔI and ΔV loop in MP&O. MP&O overpowers the disadvantages of numerous maxima by altering the step value, allowing the MPPT to correctly locate the MPP in partial shade conditions. The fluctuation and lowering of power loss end once MP&O reaches the peak value. As a result, the number of fluctuations needed and the time needed to gain the precise working point are lowered. The key distinction between P&O and MP&O in this optimization is the change in voltage and current (step size), which eliminates the drift issue.

If the irradiance value increases, the MP&O notices that dP, dV and dI are zero, and consequently duty cycle is improved by ΔDn, which is referred to as the variable step size stated by Equation (26).

$$\Delta Dn = \pm M|\Delta G| \tag{26}$$

where a constant constraint is stated as M and a change in irradiance is specified as ΔG.

Several optimization methodologies for achieving a techno-economically efficient hybrid energy system have already been developed. However, because each method has benefits and drawbacks, the model's principal goal will dictate how each strategy is implemented. Here, an advanced control technique name called IMO-MP&O, based on an EMS for a hybrid model with PV, wind, battery, and load under dynamic climate factors, can include not only variations in climatic variations but also fluctuations in load demand and battery SOC.

7. Results and Discussion

The outcomes of this research were validated using MATLAB software. MATLAB R2018a is used to implement and simulate the IMO-MP&O integrated with the HRES, which runs on a Windows 8 operating system with an Intel Core i3 processor and 4GB RAM. SimPowerSystems is used to model the inverters that use the specified control algorithms. The topology used in the simulations is explained in each of the following sections. The suggested IMO-MP&O is tested in simulations to ensure that the proposed control technique has a compensatory impact under varied irradiation situations. Tables 1–4 show the rating of PV, wind, battery, and grid employed throughout the present scheme. When combined in topologies with multiple RES coupled in series, the battery demonstrates a superior energy density. In actuality, the requirement is balanced using a battery with a comparable power density. Afterwards, the presentation and proportional study are considered in the subsequent segment.

Table 1. Rating of PV.

Constraints	Rate
Type	Sunpower SPR-305E-WHT-D
Voltage at MPP (Vmpp)	54.7
Temperature coefficient of Voc (%/deg.C)	−0.27269
Temperature coefficient of Isc (%/deg.C)	0.061745
Short-circuit current (A)	5.96
Open circuit voltage (V)	64.2
Maximum power (W)	305.226
Ideality factor	0.94504
Current at MPP (A)	5.58
Cells per module (Ncell)	96
Panel Efficiency (%)	18.7

Table 2. Rating of Wind.

Constraints	Rate
Rotational speed	1
Wind speed (m/s)	9
Magnetizing inductance (H)	7.14
Nominal output power (W)	50×10^3
Pitch angle controller gain	4
Rotor (pu)	0.047
Stator (pu)	0.048
Power Efficiency (%)	59

Table 3. Rating of Battery.

Constraints	Rate
Energy density (Wh/L)	200–250
Rated capacity (Ah)	6.7
Voltage (v)	500
Discharge Current (A)	1.4
Model	Nickel Metal Hydride
Initial State of Charge (%)	15
Fully Charged Voltage (V)	575.81
Charge/Discharge Efficiency (%)	66–92

Table 4. Rating of Grid.

Constraints	Rate
X/R ratio	5
Short circuit level	2×10^3
Voltage (Vrms)	2×10^3
Frequency (fn)	50
Base voltage	2×10^3
Active Power P (KW)	10×10^3

The execution of the proposed model is presented in Figure 4. In the simulation model, the major components are PV, wind, battery, DC-DC converter, inverter and load. Initially, the power is generated from the PV panel to grid through a DC-DC converter and inverter. If the demand is more, the turbine gets triggered and power is produced from the wind generator. Battery is used as a storage device to store the excess power. Those three sources are controlled by the hybrid technique called Improved Mayfly Optimization and Modified Perturb & Observe (IMO-MP&O) Method. From the IMO-MP&O Simulink block, the duty cycle value with step size gets generated to change the trigger the inverter switching pulse. The appropriate step size changes the duty cycle rate, enabling the PV to experience increased position and absorb peak energy. For the duration of the modeling process, the recommended program's behavior is evaluated. This framework was validated under a variety of situations and configurations of various renewable sources and a variety of customer types.

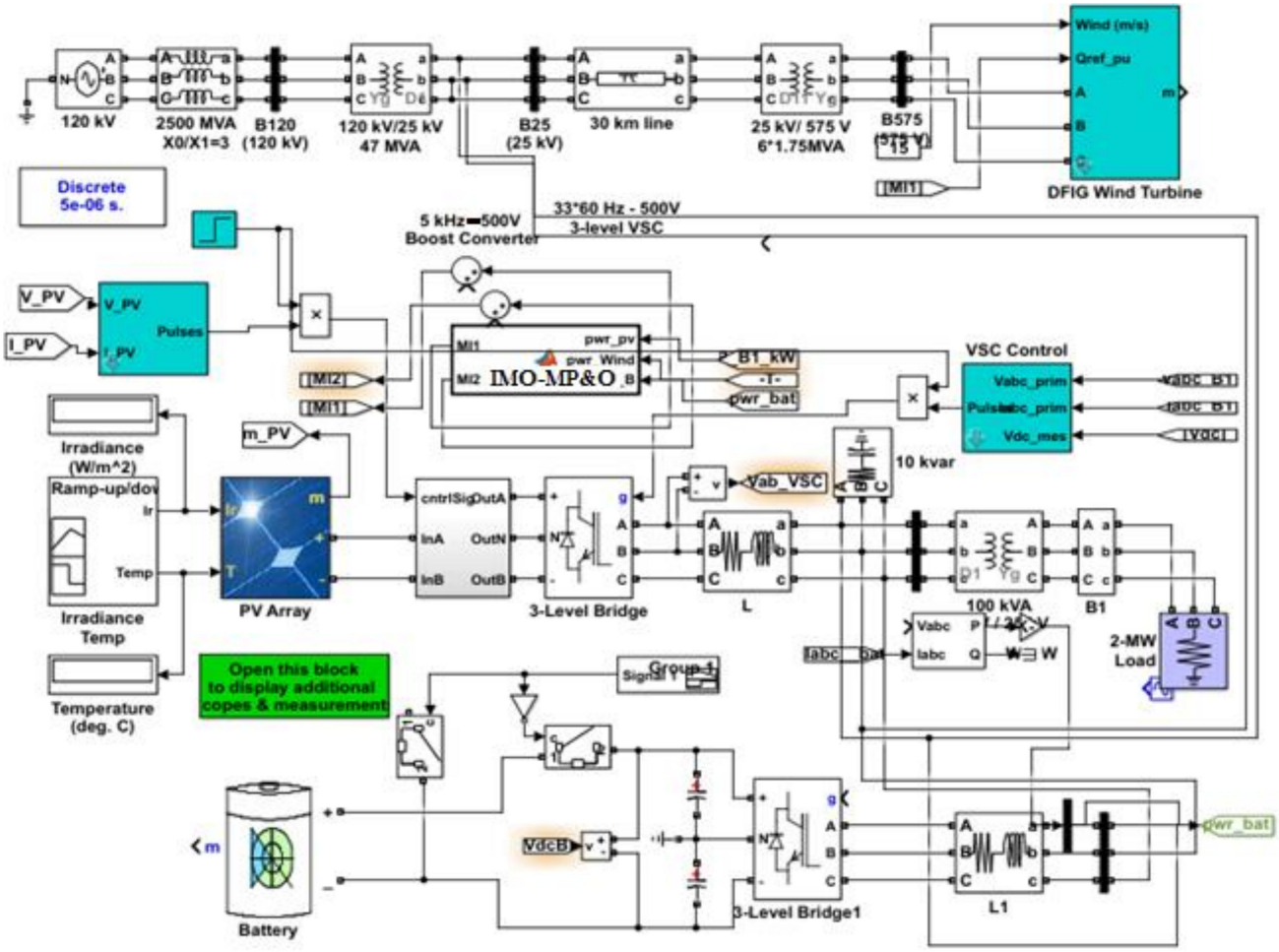

Figure 4. Simulink view of the proposed model.

7.1. Performance Study

The study of proposed IMO-MP&O in grid-integrated RES is assessed in terms of MPPT voltage/current, real/reactive power, grid voltage/current, power from PV, wind, battery and analysis THD. The proposed IMO-MP&O is compared with three combinations, such as MO-P&O, MO-MP&O and IMO-P&O. Because MO and P&O are conventional methods, by merging these two methods with different combinations, the proposed IMO-MP&O is executed and analyzed here. The mathematical model for MO, IMO, P&O and MP&O are stated in Section 6.1, 6.2 and 6.3, respectively. Furthermore, the results are plotted for three combinations (MO-P&O, MO-MP&O and IMO-P&O) and proposed IMO-MP&O method are described in the section below.

7.1.1. MPPT Voltage and Current

The MPPT voltage and current data are shown in Figures 5 and 6. With respect to both voltage and current, the IMO-MP&O is calculated using the relational controllers: P&O, IMO, and IMO-MP&O. The MPPT functionality of the PV installed in the grid-integrated RES is assessed. As shown in the statistics, the suggested IMO-MP&O controller surpasses the conventional methods in terms of MPPT effectiveness. Figures 5 and 6 show that the suggested IMO-MP&O has sophisticated MPPT current/voltage values and increased network efficiency in both static and variable modes. Owing to the existence of change in current during steady and dynamic states, the IMO-MP&O controller gives better results.

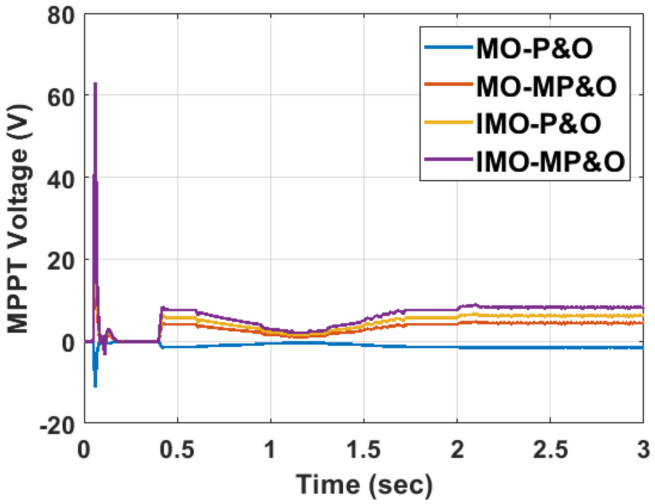

Figure 5. MPPT voltage.

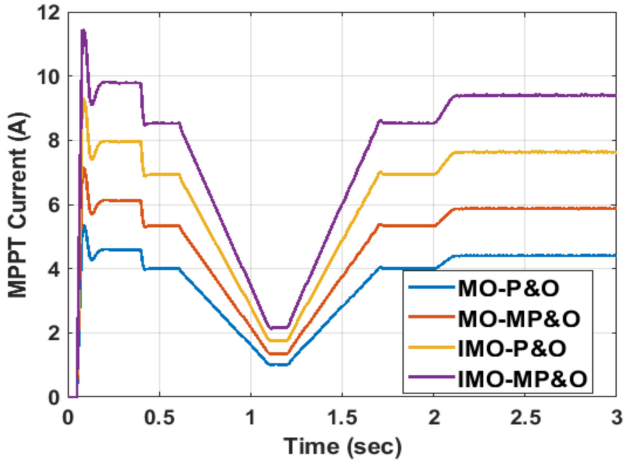

Figure 6. MPPT current.

7.1.2. Grid Voltage and Current

The entire grid voltage supplied by hybrid sources through the IMO-MP&O is shown in Figure 7. Figure 7 shows how the grid voltage increased at random moments depending on the point of common coupling variance. Based on the findings, it can be concluded that changes in sun illumination have a greater impact on electricity production than variations in weather.

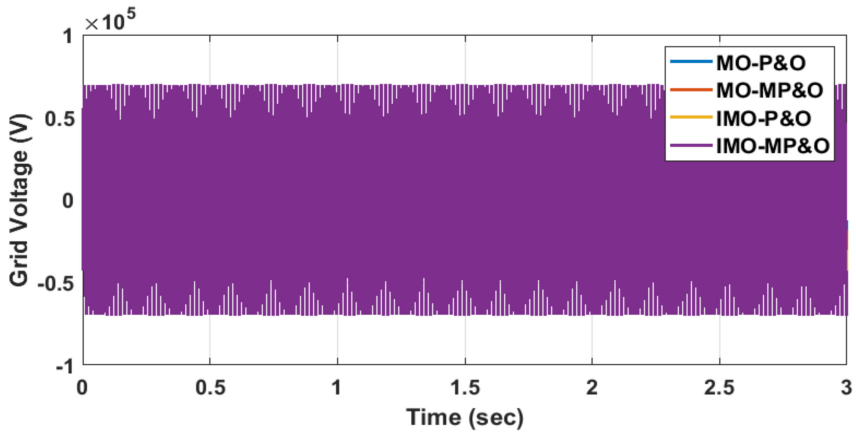

Figure 7. Grid voltage.

The terminal voltage is originally greater than the requirement during moderate irradiation values. The voltage level, across the other side, will be less than the need for zero or quite a moderate illumination. In the same diagram, this is depicted as negative energy. The supply from the network is shown as negative energy, whilst the PV power delivery to the grid is shown as positive power. Figure 8 shows the grid voltage provided between 1.35 and 1.65 s. Figure 8 shows that the recommended IMO-MP&O delivers greater voltage levels to balance the generation capacity when compared to the other three conventional controllers.

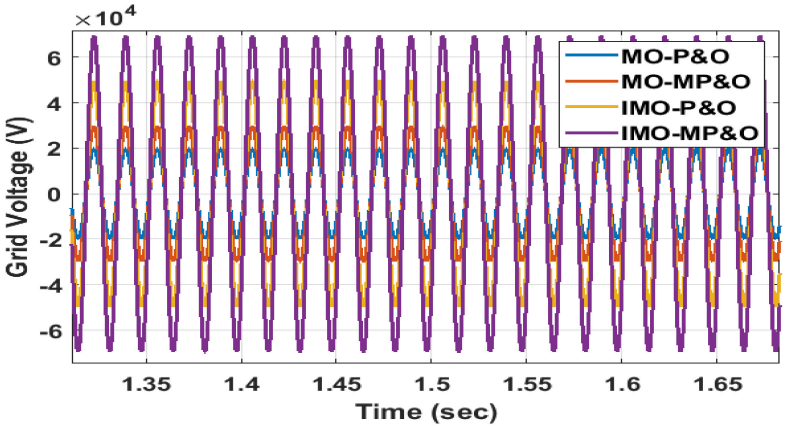

Figure 8. Grid voltage between 1.35 s and 1.65 s.

Figure 9 shows the total grid current given to the grid system, whereas Figure 10 shows the current delivered between 0.9 s and 1.4 s. During varying levels of illumination, the module creates increased grid current and voltage, resulting in greater grid electricity. MPPT chooses MPP from the starting point using an IMO-MP&O controller. This also explains how the designed RES, through IMO-MP&O, can meet peak loads. The created structure is essentially practical extensive simulation findings of stable and unstable testing. Furthermore, the model has been used to investigate the dynamic response of HRES with a significant electricity content.

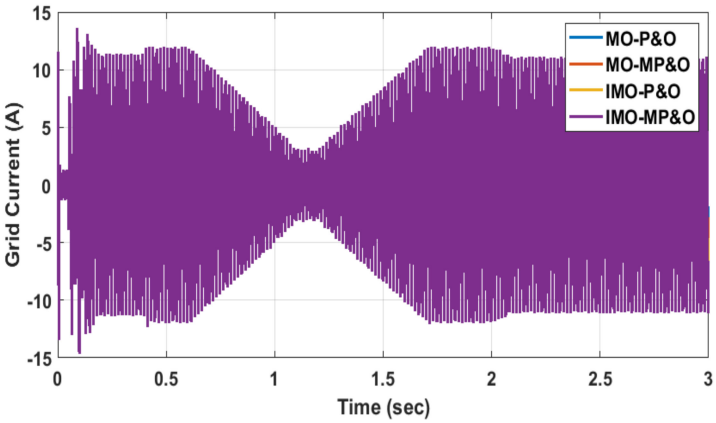

Figure 9. Grid current.

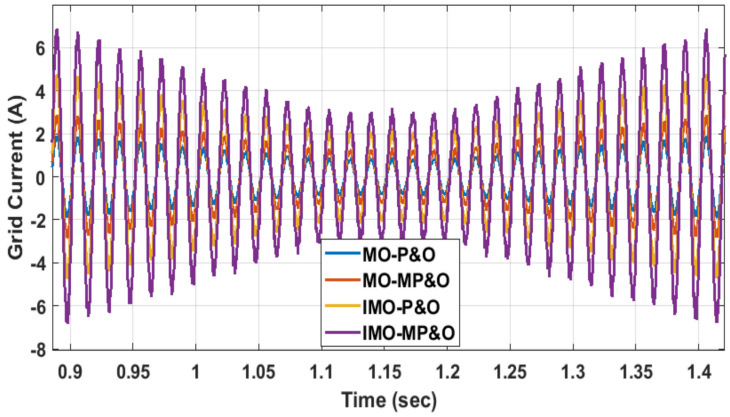

Figure 10. Grid current between 0.9 s and 1.4 s.

7.1.3. Real Power and Reactive Power

The real power and reactive power obtained through the transmission line are depicted in Figures 11 and 12, respectively. The amount of active power produced by hybrid sources while utilizing the IMO-MP&O is greater than the average power produced by conventional methods, as shown in Figures 11 and 12.

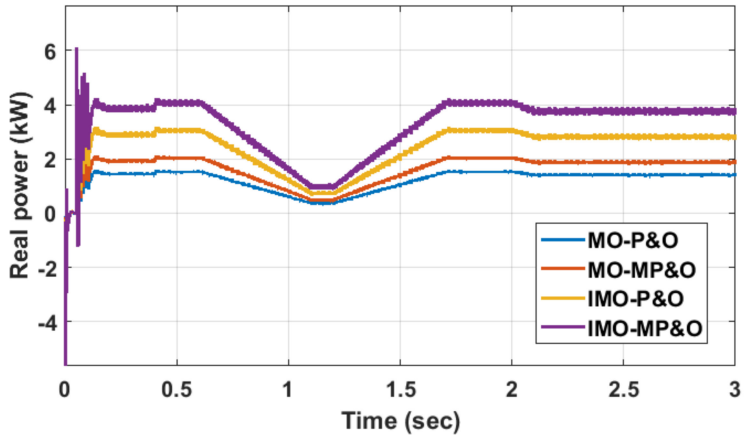

Figure 11. Performance of Real power.

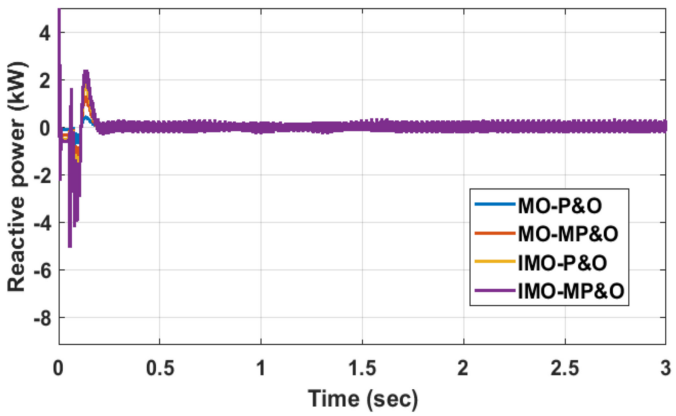

Figure 12. Performance of Reactive power.

As a result, the created IMO-MP&O meets the grid's greater power requirements. The use of IMO to manage the shifting of the wind and batteries helps to reduce the distortions produced by the power converters. An IMO-dependent transitioning strategy is utilized to boost the power while reducing distortions. Furthermore, surplus power from the primary

source is utilized to recharge the backup storage, which can only be used as a reserve while both the PV and the wind are unable to transmit electricity. The RES provides reactive power flow in the range of 0.06 s to 0.24 s, as shown in Figure 13.

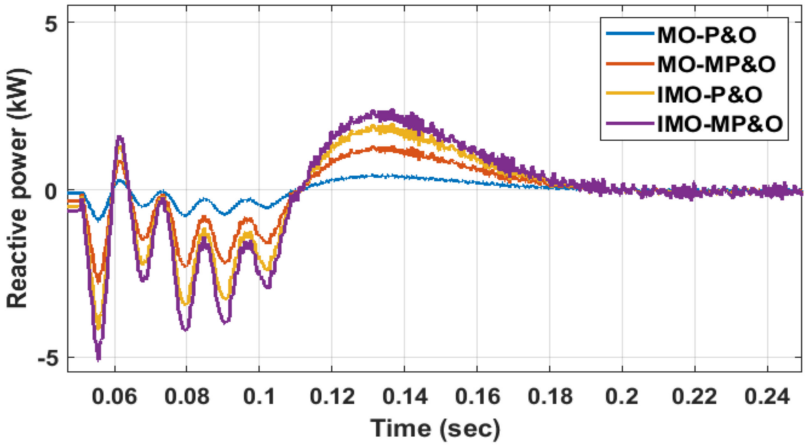

Figure 13. Reactive power between 0.06 s and 0.24 s.

7.1.4. Performance of Power Generation

In this subsection, the power from all sources is depicted. Total power from the PV panel, wind, and battery should be checked in the IMO-MP&O block. It generates the modulation index value by testing the power. That number is used to refer to both the wind and battery sections. The output power is altered, and the load demand is compensated based on the reference value. Figure 14 shows a power comparison chart for the existing and proposed methods.

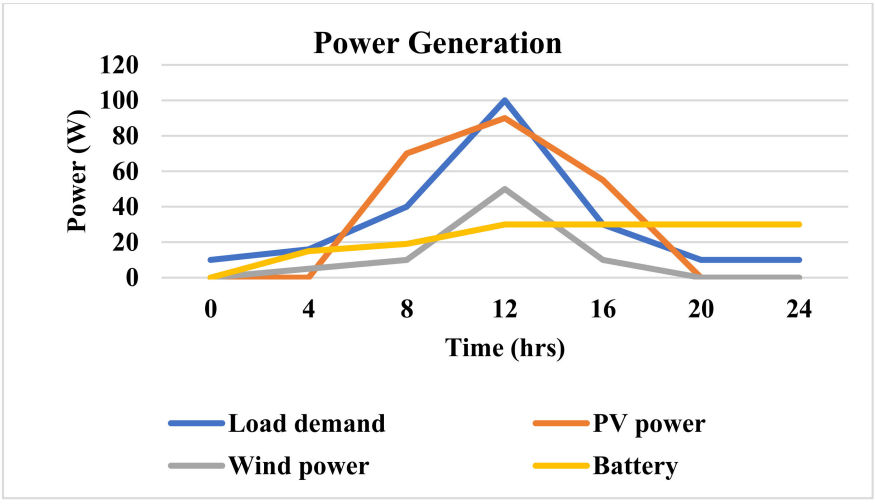

Figure 14. Overall Power Generation.

7.1.5. Performance of THD

THD is caused by a variety of factors, including the converter's DC signal, various load requirements, improper transition management, and low illumination levels. To reduce the fluctuations in received power, capacitors are controlled and installed among the load as well as the generator in this research. The graphical representation of THD using MO-P&O under linear load is shown in Figure 15. From the Figure 15, it clearly shows that MO-P&O attains the THD of 1.36%. To meet non-linear power demands, MO-MP&O and IMO-P&O is employed to reduce the THD as 1.32% and 0.92% which is shown in Figures 16 and 17; In order to provide a suitable arrangements to the respective sources (wind and battery)

throughout fluctuating system load, proposed IMO-MP&O is applied to achieve less THD of 0.77% which is displayed in Figure 18.

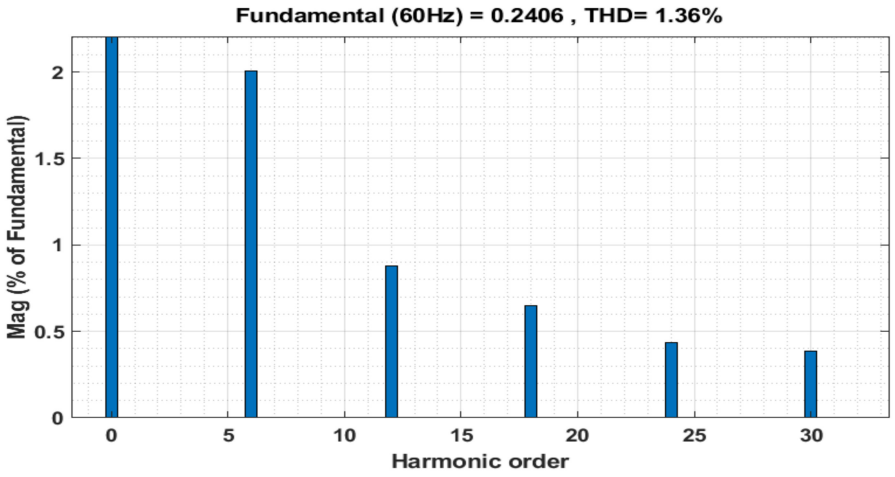

Figure 15. THD for MO-P&O.

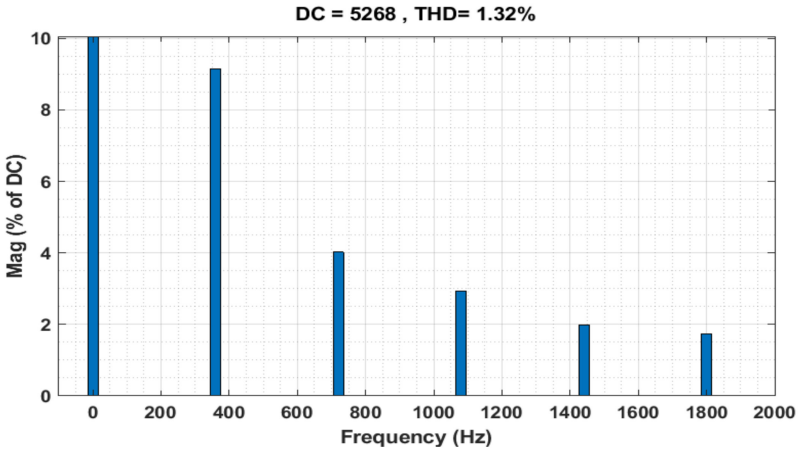

Figure 16. THD for MO-MP&O.

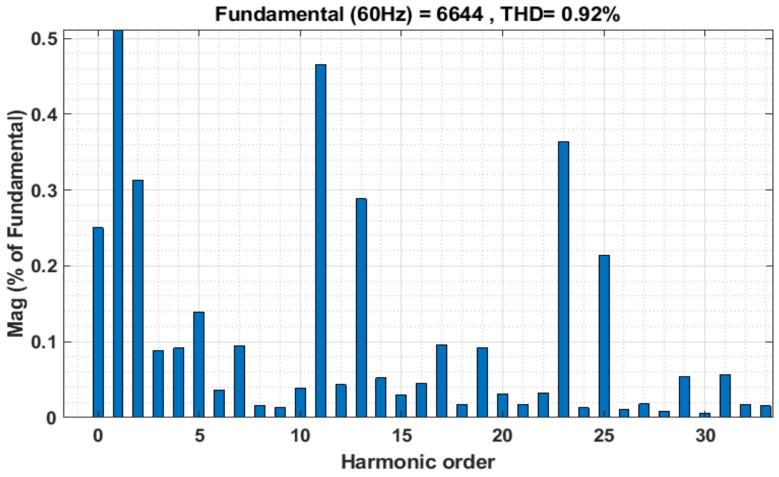

Figure 17. THD for IMO-P&O.

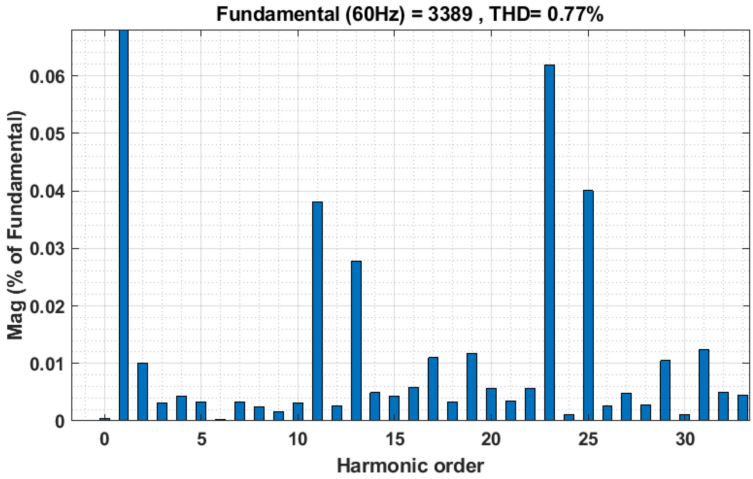

Figure 18. THD for IMO-MP&O.

7.2. Comparative Analysis

When comparing the grid integrated renewable source through the IMO-MP&O to conventional RES systems, the performance of hybrid resources through IMO-MP&O is demonstrated. The designed IMO-MP&O is associated with existing MPPT [26] control. The designed IMO-MP&O and traditional MPPT Control [26] are compared in Table 5.

Table 5. Comparative Analysis of Power.

Conditions	Time (Min)	PV Power (W)		Wind Power (W)		Battery Power (W)	
		MPPT Controller [26]	Proposed IMO-MP&O	MPPT Controller [26]	Proposed IMO-MP&O	MPPT Controller [26]	Proposed IMO-MP&O
Radiation-1000, Temperature—35′ Wind Speed—9 m/s.	8.30–9.20	50	79.37	35	65.97	2	29.97
	9.30–10.20	54.26	82.93	42.18	66.24	−22.2	5.80
	10.30–11.20	54.26	83.91	42.18	67.81	−43.14	0.99
	11.30–12.20	54.26	83.99	42.18	68.23	−43.14	8.08
	12.30–1.20	54.26	84.36	42.18	68.88	−22.17	10.20
	1.30–2.20	54.26	84.83	42.18	69.34	2.9	18.40
	2.30–3.20	54.26	86.27	42.18	71.55	16.13	26.87
	3.30–4.20	54.26	86.27	42.18	71.55	22.24	29.98

Environmental circumstances affect the electrical power generated by renewable sources such as wind and solar power, causing problems in the load sector. The amount of power created by solar energy changes when there is no sun or when the weather is gloomy. As a result, wind does not always blow at the same pace; it is intermittent. The amount of power generated from the renewable sources will be changeable. As load conditions change, power is delivered from hybrid sources. The excess power from the sources is stored in backup batteries; sometimes power from batteries is supplied to other small loads under variable load conditions. Therefore, load conditions do not affect the performance of the proposed method.

Table 5 shows the comparative analysis of power generated from HRES. Table 5 obviously designates that the suggested IMO-MP&O accomplishes better power generation in all the conditions when compared with the existing MPPT controller [26], which attains less power generation.

Figure 19 depicts a graphical representation of the THD comparison. Table 6 shows the results of the THD comparison. Harmonics are present in the magnitude component of ANN-Z-Source [28] control methods when the input signal contains both DC offset and noise when phase 'a' of the load is removed. The suggested IMO-MP&O control, on the other hand, estimates less harmonics, 0.77%.

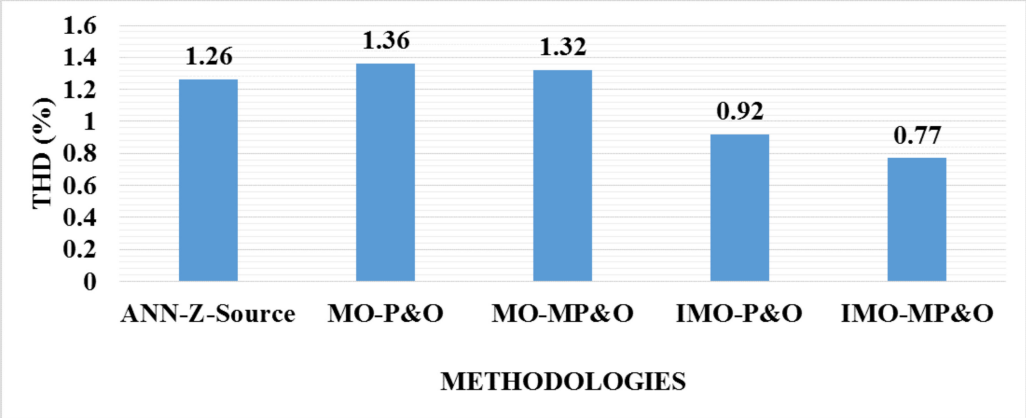

Figure 19. Comparison of THD.

Table 6. Comparative Analysis of THD.

Techniques	THD (%)
ANN-Z-Source [28]	1.26
MO-P&O	1.36
MO-MP&O	1.32
IMO-P&O	0.92
IMO-MP&O	0.77

8. Conclusions

In this study, a hybrid system was made up of two renewable energy sources: photovoltaic (PV) and wind energy (WE), a battery bank and a variable load. The main goals were to regulate the hybrid model power such that total requirements were satisfied and prolonged the recharging period by keeping the *SOC* within definite limits to minimize a shutdown. The IMO-MP&O approach was used to construct an effective EMS using a PV/wind/battery system in this research. The modulation index from the suggested IMO-MP&O approach was used to govern an effective switching between battery and wind. A centralized management algorithm (IMO-MP&O) is designed to control the energy flows among the hybrid system's components and to determine the best operating mode for ensuring a constant flow of the load with minimal battery usage. The effectiveness and results of the proposed control methods are demonstrated using simulation results obtained in the Matlab/Simulink environment. For validation purposes, the proposed IMO-MP&O controller was employed in the grid-connected RES system under various irradiance and temperature levels. The main benefit of this proposed IMO-MP&O was a better convergence rate while there is a change in current, which produces an effective EMS for PV/wind/battery systems. The results demonstrate that the proposed IMO-MP&O generates more electricity and has a THD of 0.77% when compared to the existing ANN-Z-Source converter, which attains 1.26%. This research work can be extended in the future to test the EMS under various climatic circumstances using various hybrid approaches.

Author Contributions: The paper investigation, resources, data curation, writing—original draft preparation, writing—review and editing, and visualization were done by P.S. and S.M. The paper conceptualization, software, were conducted by D.R. The validation and formal analysis, methodology, supervision, project administration, and funding acquisition of the version to be published were conducted by W.-C.L. All authors have read and agreed to the published version of the manuscript.

Funding: This research received no external funding.

Institutional Review Board Statement: Not applicable.

Informed Consent Statement: Not applicable.

Data Availability Statement: Not applicable.

Conflicts of Interest: The authors declare no conflict of interest.

References

1. Ali, I.B.; Turki, M.; Belhadj, J.; Roboam, X. Systemic design and energy management of a standalone battery-less PV/Wind driven brackish water reverse osmosis desalination system. *Sustain. Energy Technol. Assess.* **2020**, *42*, 100884.
2. Ahmed, F.; Kaaniche, K.; Alanazi, T.M. Recent approach based social spider optimizer for optimal sizing of hybrid PV/wind/battery/diesel integrated microgrid in aljouf region. *IEEE Access* **2020**, *8*, 57630–57645.
3. Murty, V.V.S.N.; Kumar, A. Multi-objective energy management in microgrids with hybrid energy sources and battery energy storage systems. *Prot. Control. Mod. Power Syst.* **2020**, *25*, 2. [CrossRef]
4. Yu, D.; Zhang, T.; He, G.; Nojavan, S.; Jermsittiparsert, K.; Ghadimi, N. Energy management of wind-PV-storage-grid based large electricity consumer using robust optimization technique. *J. Energy Storage* **2020**, *27*, 101054. [CrossRef]
5. Meisam, F.; Aghdam, F.H.; Alahyari, A.; Monavari, A.; Safari, A. Optimal energy management and sizing of renewable energy and battery systems in residential sectors via a stochastic MILP model. *Electr. Power Syst. Res.* **2020**, *187*, 106483.
6. Chakir, A.; Tabaa, M.; Moutaouakkil, F.; Medromi, H.; Julien-Salame, M.; Dandache, A.; Alami, K. Optimal energy management for a grid connected PV-battery system. *Energy Rep.* **2020**, *206*, 218–231. [CrossRef]
7. Lai, W.-C.; Jian, R.; Xin, X. DC-DC Converter and Rectifier with Resonator for Underwater Wireless Power Transfer Module. In Proceedings of the 2020 IEEE International Conference on Consumer Electronics—Taiwan (ICCE-Taiwan), Taoyuan, Taiwan, 28–30 September 2020.
8. Lai, W.-C. DC-DC Converter and Rectifier with Resonator for Solar and Wireless Charging in Advanced Driver Assistance Systems. In Proceedings of the 2019 IEEE 4th International Future Energy Electronics Conference (IFEEC), Singapore, 25–28 November 2019.
9. Shivam, K.; Tzou, J.; Wu, S. A multi-objective predictive energy management strategy for residential grid-connected PV-battery hybrid systems based on machine learning technique. *Energy Convers. Manag.* **2021**, *237*, 114103. [CrossRef]
10. Oussama, H.; Othmane, A.; Mohammed Amine, H.; Abdesselam, C.; Mohammed Amine, S. Proposed energy management for a decentralized DC-microgrid based PV-WT-HESS for an isolated community. *Int. J. Power Electron. Drive Syst.* **2020**, *11*, 2073. [CrossRef]
11. Mahfuz-Ur-Rahman, A.M.; Islam, M.; Muttaqi, K.M.; Sutanto, D. An effective energy management with advanced converter and control for a PV-battery storage based microgrid to improve energy resiliency. *IEEE Trans. Ind. Appl.* **2021**, *57*, 6659–6668. [CrossRef]
12. Benlahbib, B.; Bouarroudj, N.; Mekhilef, S.; Abdeldjalil, D.; Abdelkrim, T.; Bouchafaa, F. Experimental investigation of power management and control of a PV/wind/fuel cell/battery hybrid energy system microgrid. *Int. J. Hydrog. Energy* **2020**, *45*, 29110–29122. [CrossRef]
13. Sahri, Y.; Belkhier, Y.; Tamalouzt, S.; Ullah, N.; Nath Shaw, R.; Chowdhury, M.; Techato, K. Energy Management System for Hybrid PV/Wind/Battery/Fuel Cell in Microgrid-Based Hydrogen and Economical Hybrid Battery/Super Capacitor Energy Storage. *Energies* **2021**, *14*, 5722. [CrossRef]
14. Ismail, M.M.; Bendary, A.F.; Elsisi, M. Optimal design of battery charge management controller for hybrid system PV/wind cell with storage battery. *Int. J. Power Energy Convers.* **2020**, *11*, 412–429. [CrossRef]
15. Elmorshedy, M.F.; Elkadeem, M.R.; Kotb, K.M.; Taha, I.B.M.; Mazzeo, D. Optimal design and energy management of an isolated fully renewable energy system integrating batteries and supercapacitors. *Energy Convers. Manag.* **2021**, *245*, 114584. [CrossRef]
16. Murty, V.V.V.S.N.; Kumar, A. Optimal energy management and techno-economic analysis in microgrid with hybrid renewable energy sources. *J. Mod. Power Syst. Clean Energy* **2020**, *8*, 929–940. [CrossRef]
17. Kafetzis, A.; Ziogou, C.; Panopoulos, K.D.; Papadopoulou, S.; Seferlis, P.; Voutetakis, S. Energy management strategies based on hybrid automata for islanded microgrids with renewable sources, batteries and hydrogen. *Renew. Sustain. Energy Rev.* **2020**, *134*, 110118. [CrossRef]
18. Rathish, R.J.; Mahadevan, K.; Selvaraj, S.K.; Booma, J. Multi-objective evolutionary optimization with genetic algorithm for the design of off-grid PV-wind-battery-diesel system. *Soft Comput.* **2021**, *25*, 3175–3194. [CrossRef]
19. Al-Quraan, A.; Al-Qaisi, M. Modelling, Design and Control of a Standalone Hybrid PV-Wind Micro-Grid System. *Energies* **2021**, *14*, 4849. [CrossRef]
20. Azaroual, M.; Ouassaid, M.; Maaroufi, M. An optimal energy management of grid-connected residential photovoltaic-wind-battery system under step-rate and time-of-use tariffs. *Int. J. Renew. Energy Res.* **2020**, *10*. [CrossRef]
21. Abdelshafy, A.M.; Jurasz, J.; Hassan, H.; Mohamed, A.M. Optimized energy management strategy for grid connected double storage (pumped storage-battery) system powered by renewable energy resources. *Energy* **2020**, *192*, 116615. [CrossRef]
22. Hemeida, A.M.; El-Ahmar, M.H.; El-Sayed, A.M.; Hasanien, H.M.; Alkhalaf, S.; Esmail, M.F.C.; Senjyu, T. Optimum design of hybrid wind/PV energy system for remote area. *Ain Shams Eng. J.* **2020**, *11*, 11–23. [CrossRef]
23. Elkazaz, M.; Sumner, M.; Thomas, D. Energy management system for hybrid PV-wind-battery microgrid using convex programming, model predictive and rolling horizon predictive control with experimental validation. *Int. J. Electr. Power Energy Syst.* **2019**, *115*, 105483. [CrossRef]

24. Jha, S.K.; Kumar, D. Assessment of Battery Energy Storage System with Hybrid Renewable Energy Sources to Voltage Control of Islanded Microgrid Considering Demand-Side Management Capability. *Iran. J. Sci. Technol. Trans. Electr. Eng.* **2020**, *44*, 861–877. [CrossRef]
25. Padhmanabhaiyappan, S.; Karthik, R.; Ayyar, K. Optimal utilization of interconnected RESs to microgrid: A hybrid AWO-ANFIS technique. *Soft Comput.* **2019**, *24*, 10493–10513. [CrossRef]
26. Kumar, P.; Satish, R.P.; Chandrasena, S.; Ramu, V.; Srinivas, G.N.; Victor Sam Moses Babu, K. Energy management system for small scale hybrid wind solar battery based microgrid. *IEEE Access* **2020**, *8*, 8336–8345. [CrossRef]
27. Al Alahmadi, A.A.; Belkhier, Y.; Ullah, N.; Abeida, H.; Soliman, M.S.; Hassan Khraisat, Y.S.; Mohammed Alharbi, Y. Hybrid wind/PV/battery energy management-based intelligent non-integer control for smart DC-microgrid of smart university. *IEEE Access* **2021**, *9*, 98948–98961. [CrossRef]
28. Santhoshi, B.K.; Mohanasundaram, K.; Ashok Kumar, L. ANN-based dynamic control and energy management of inverter and battery in a grid-tied hybrid renewable power system fed through switched Z-source converter. *Electr. Eng.* **2021**, *103*, 2285–2301. [CrossRef]
29. De, M.; Das, G.; Mandal, K.K. An effective energy flow management in grid-connected solar–wind-micro-grid system incorporating economic and environmental generation scheduling using a meta-dynamic approach-based multi-objective flower pollination algorithm. *Energy Rep.* **2021**, *7*, 2711–2726. [CrossRef]
30. Jain, A.A.; Rabi, B.J.; Darly, S.S. Application of QOCGWO-RFA for maximum power point tracking (MPPT) and power flow management of solar PV generation system. *Int. J. Hydrogen Energy* **2019**, *45*, 4122–4136. [CrossRef]
31. Revathy, S.R.; Kirubakaran, V.; Rajeshwaran, M.; Balasundaram, T.; Sekar, V.S.; Alghamdi, S.; Rajab, B.S.; Babalghith, A.O.; Anbese, E.M. Design and Analysis of ANFIS–Based MPPT Method for Solar Photovoltaic Applications. *Int. J. Photoenergy* **2022**, *2022*, 9625564. [CrossRef]
32. Nyeche, E.N.; Diemuodeke, E.O. Modelling and optimisation of a hybrid PV-wind turbine-pumped hydro storage energy system for mini-grid application in coastline communities. *J. Cleaner Prod.* **2019**, *250*, 119578. [CrossRef]
33. Hamanah, W.M.; Abido, M.A.; Alhems, L.M. Optimum Sizing of Hybrid PV, Wind, Battery and Diesel System Using Lightning Search Algorithm. *Arab. J. Sci. Eng.* **2019**, *45*, 1871–1883. [CrossRef]
34. Mo, S.; Ye, Q.; Jiang, K.; Mo, X.; Shen, G. An improved MPPT method for photovoltaic systems based on mayfly optimization algorithm. *Energy Rep.* **2022**, *8*, 141–150. [CrossRef]